

Supplementary Information

for

Fast removal of aqueous Hg(II) with quaternary ammonium-functionalized magnetic mesoporous silica and regeneration

Jinshui Liu^{ab} and Xuezhong Du^{*a}

^aKey Laboratory of Mesoscopic Chemistry (Ministry of Education), School of Chemistry and Chemical Engineering, Nanjing University, Nanjing 210093, P. R. China. E-mail: xzdu@nju.edu.cn. Fax: 86-25-83317761

^bAnhui Key Laboratory of Functional Molecular Solids, College of Chemistry and Materials Science, Anhui Normal University, Wuhu 241000, P. R. China

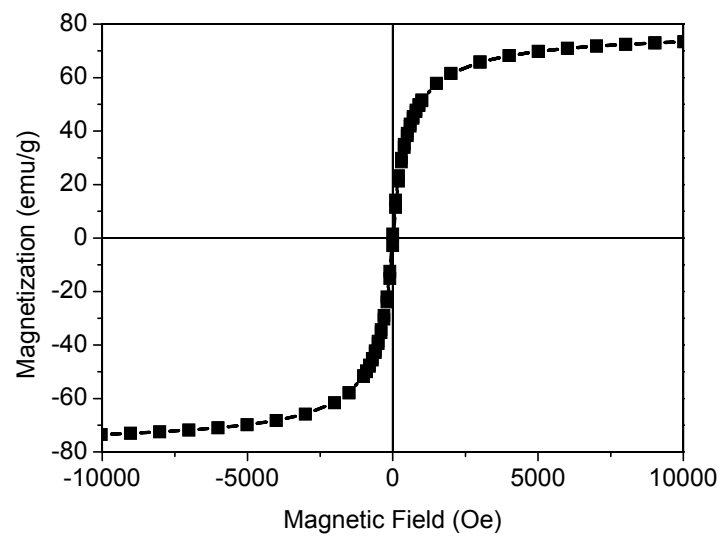


Fig. S1 Field-dependent magnetization curves of Fe_3O_4 nanoparticles at 300 K.

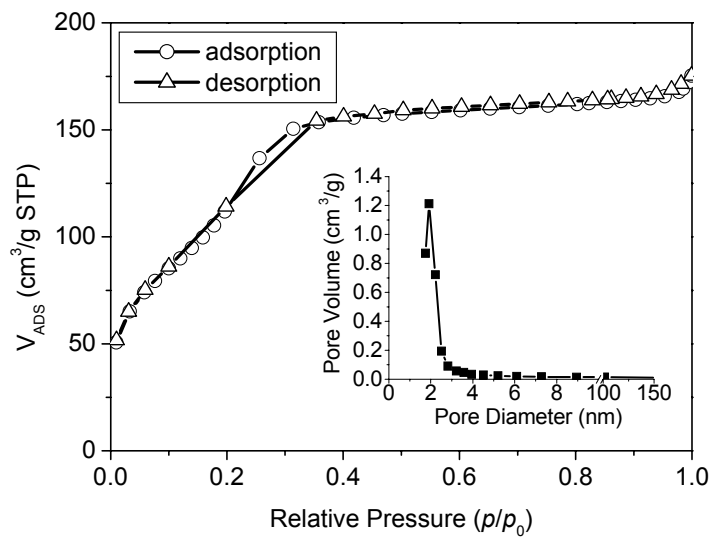


Fig. S2 Nitrogen adsorption–desorption isotherms of AMMS. The inset shows pore size distribution of AMMS.

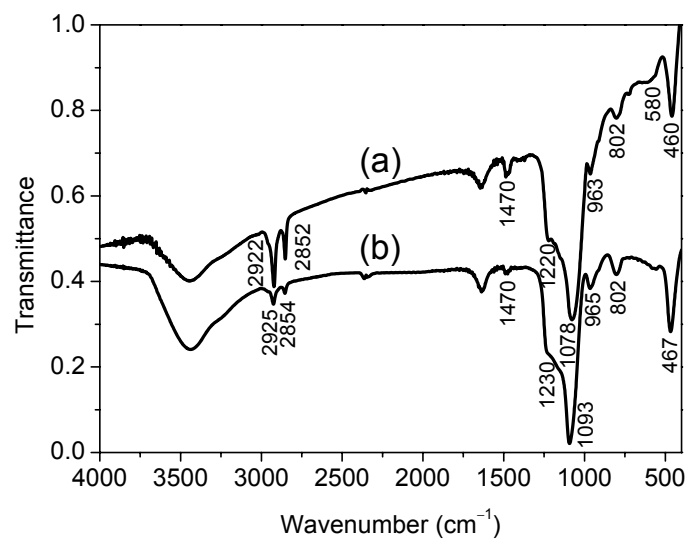


Fig. S3 FTIR spectra of AMMS: (a) before surfactant extraction; (b) after surfactant extraction.

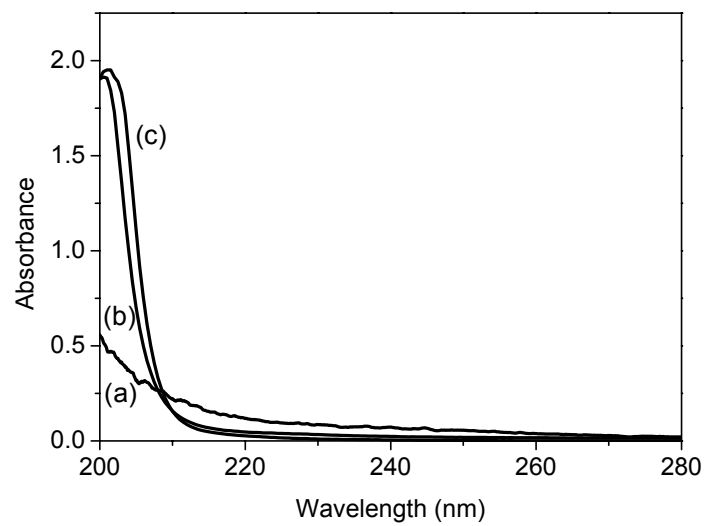


Fig. S4 UV-vis spectra of (a) PDDA (0.01 mol/L), (b) BTAC (0.20 mol/L), (c) NaCl (0.25 mol/L).

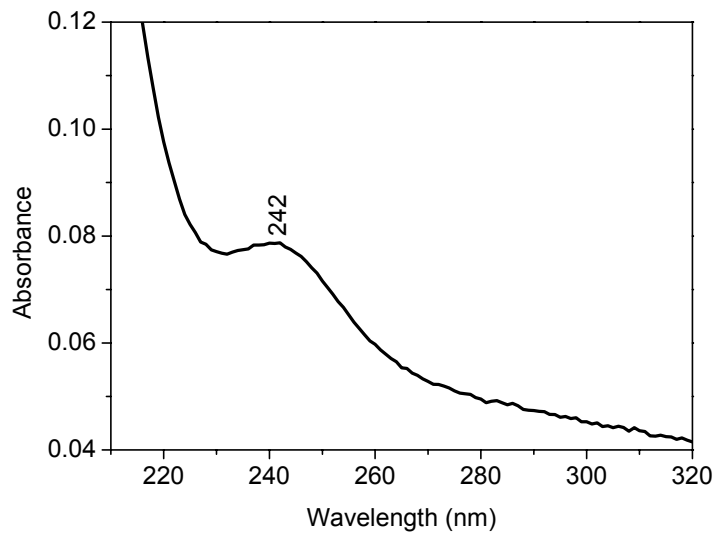


Fig. S5 UV-vis spectrum of a TTAC-functionalized quartz plate after Hg(II) adsorption with a counterpart before Hg(II) adsorption as a reference.

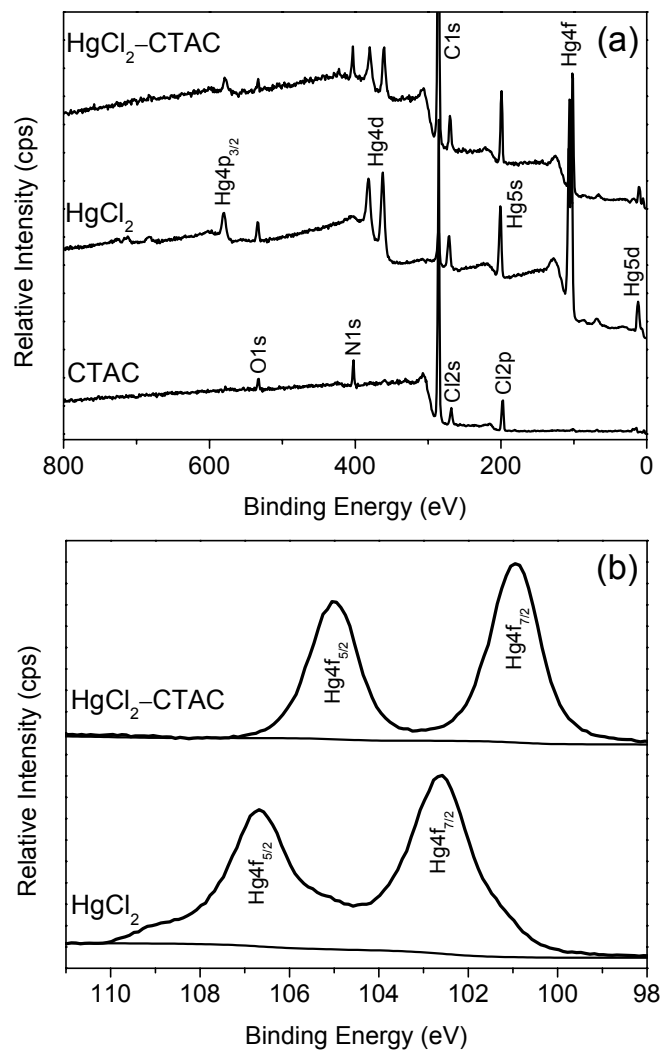


Fig. S6 XPS spectra of CTAC, HgCl₂, and CTAC complex with HgCl₂: (a) survey scans; (b) high-resolution scans in the regions of Si2p and Hg4f binding energies

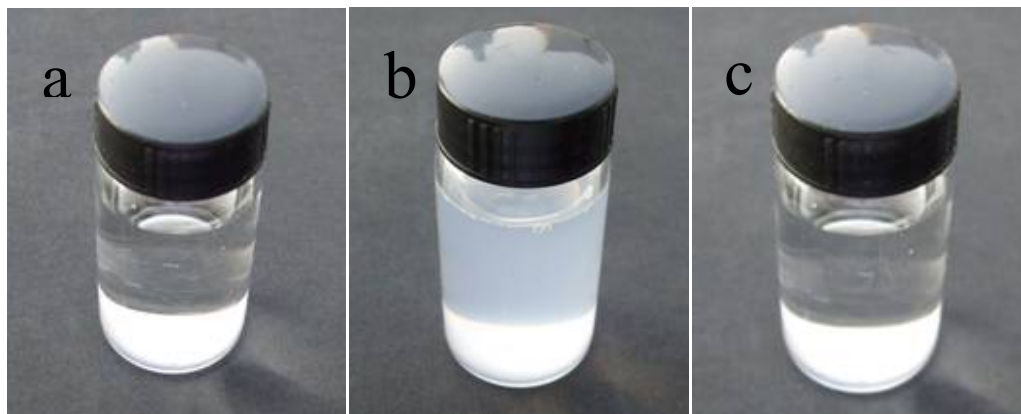


Fig. S7 Photographs of vials containing aqueous CTAC solution (1 mmol/L) in the absence or presence of HgCl₂ (0.085 mmol/L) at different pH: (a) none, pH 5.5; (b) HgCl₂, pH 5.5; (c) HgCl₂, pH 8.5.